SECOND EUROPEAN CONFERENCE ON EARTHQUAKE ENGINEERING
AND SEISMOLOGY, ISTANBUL AUG. 25-29, 2014

ON THE DEFORMATION CAPACITY OF CONCENTRICALLY STEEL BRACES

Omid SEDEHI[1] and Hassan MOGHADDAM[2]

ABSTRACT

In this paper, the current provisions for seismic design of concentric steel braces are reviewed. Due to these provisions, the overall deformation capacity predominantly depends on the overall slenderness ratio representing the overall buckling. However, in many cases this may not hold true as the local buckling becomes the predominant cause of rupture. Finite Element (FE) analysis is carried out to investigate the behaviour of steel braces subjected to cyclic loadings. These models proved to be capable of predicting the formation of plastic hinge, and the occurrence of overall and local buckling at the mid-span with reasonable accuracy. Measurement of the strain at the mid-span plastic hinge demonstrates a sharp rise after the occurrence of local buckling. This severe growth of strain results in the rupture failure at the mid-span plastic hinge, as confirmed by the general observations in experiments. As a result, the local buckling is identified and introduced as the main limit state that can be used as an index for evaluation of the overall deformation capacity of braces. The difference between strains at outer and inner layers of the shell elements located at the mid-span is introduced as an index for detecting the occurrence of local buckling. This index could be employed to quantify the overall axial deformation that produces local buckling.

INTRODUCTION

Concentrically steel braced frames (CBF) are a common type of lateral load resisting systems. Tubular members, pipes and hollow structural shapes (HSS), have been frequently used as CBFs. Seismic performance of tubular braces greatly depends on slenderness ratio, and width-to-thickness ratio. Usage of braces with lower slenderness ratio might postpone overall buckling, and obtain higher compression strength. However, such braces exhibited less ductile fracture behaviour in experiments (Tremblay 2002).

Overall compression loading triggers two inevitable geometric changes entitled as overall and local buckling. The overall buckling causes a reduction in load carrying capacity, although the member can still experience further inelastic deformations. On the contrary, there is no reduction in load carrying capacity to be identified as occurrence of local buckling, and nevertheless, the local buckling deteriorates deformation capacity. Thus, the local buckling is not detectable compared to the overall buckling. The occurrence of local buckling depends on the compactness of braces, and more compacted members can experience further inelastic deformations (Elchalakani et al. 2003; Fell 2008).

Experimental investigations showed that cyclic loading forms a plastic hinge at the mid-span, and another one at each end of the brace (Haddad 2004). Formation of plastic hinge at the mid-span is accompanied by concentration of stress and strain (Han et al. 2007). Strain concentration sharply rises after the occurrence of local buckling resulted in a rupture failure at the mid-span (Haddad 2004). In

[1] PhD student, Sharif University of Technology, Tehran, Iran, sedehi-omid@outlook.com
[2] Professor, Sharif University of Technology, Tehran, Iran, hsnmoghaddam@yahoo.com

addition, the formation of plastic hinge at the each end might result in net section fracture of braces (Astaneh-Asl et al. 1985; Fell 2008). In summary, two main rupture modes can be specified for tubular members; rupture failure at the mid-span, and net section fracture. Han et al. (2007) observed that the net section fracture is not a ductile fracture mechanism as opposed to rupture failure due to the local buckling.

In this paper, a review on design provisions of CBFs was carried out to assess deformation capacity of tubular braces. Parameters which were considered as main effective ones in AISC 341 (2010) and ASCE 41 (2007) were identified and compared with previous studies. Furthermore, finite element (FE) analyses were carried out to investigate behaviour of tubular braces subjected to cyclic loading. For this purpose and to verify analytical results, four previously tested tubular braces were selected to obtain FE models. The occurrence of overall and local buckling, the formation of plastic hinges, strain concentration, and effects of cyclic loading were investigated in detail.

DESIGN PROVISIONS

AISC 341 (2010) generally categorised CBFs to special concentrically braced frame (SCBF), and ordinary concentrically braced frame (OCBF). The major difference between these two categories is that SCBFs can experience much more inelastic deformation in comparison with OCBFs. In other words, SCBFs can experience inelastic deformations through yield, and overall buckling while OCBFs are expected to remain elastic. AISC 341 (2010) limits the slenderness ratios, and width-to-thickness ratios, as presented in Table.1.

Table 1. Limits to design of CBFs (AISC 2010)

Section Type	Width/diameter-to-thickness ratio		Slenderness ratio	
	SCBF	OCBF	SCBF	OCBF
SHSS[a]	$\frac{b}{t} \le 0.55\sqrt{\frac{E}{F_y}}$	$\frac{b}{t} \le 0.64\sqrt{\frac{E}{F_y}}$	$\frac{KL}{r} \le 200$	$\frac{KL}{r} \le 4\sqrt{\frac{E}{F_y}}$ [c]
CHS[b]	$\frac{d}{t} \le 0.038\frac{E}{F_y}$	$\frac{d}{t} \le 0.044\frac{E}{F_y}$	$\frac{KL}{r} \le 200$	$\frac{KL}{r} \le 4\sqrt{\frac{E}{F_y}}$ [c]

a. SHSS i.e., square hollow structural shapes
b. CHS i.e., circular hollow sections
c. Slenderness ratio of OCBF is only restricted for V-Braced, or inverted V-Braced.

In Table.1, E is modulus of elasticity, and F_y is yield stress. The major purpose of limiting width-to-thickness ratio and slenderness ratio is to increase the bracings' resistance against the occurrence of local and overall buckling, respectively. However, meeting AISC's requirements merely postpones buckling. Furthermore, such provisions are generally on the conservative side, and were attempted to provide acceptable capability to experience inelastic deformations.

Although the main purpose of limiting geometric properties was to provide adequate deformation capacity, a displacement based design method was not suggested in AISC 341 (2010). ASCE 41 (2007) explained the deformation capacity of braces in terms of axial displacement corresponding to overall buckling (Δ_c) and axial yield deformation (Δ_T). Table.2 gives the deformation capacities in the case of tubular braces. According to table.2, the deformation capacity of braces in compression generally depends on the overall buckling deformation (Δ_c) which can be determined from the following relationship:

$$\Delta_c = \frac{P_B L}{EA} \tag{1}$$

where P_B is overall buckling load, L is total length of brace, E is elastic modulus, and A is cross-sectional area. Referring to Table.2, the corresponding deformation capacity of slender braces is recommended higher than stocky ones. On the contrary, an increase in slenderness ratio results in reduction of the overall buckling load, and this in turn will be resulted in reduction of the deformation capacity of braces in compression. Therefore, it can be pointed out that the effect of slenderness ratio on deformation capacity might be overlooked in ASCE 41 (2007). However, previous experiments represented that braces with larger slenderness ratios show more ductile behaviour in comparison with stocky ones (Tremblay et al. 2003; Fell 2008).

Table 2. Deformation capacity of tubular braces under compression and tension (ASCE 41 2007)

Component/Action type	Deformation Capacity		
	Acceptance Criteria		
	IO[a]	LS[b]	CP[c]
Stocky HSS, Pipes, Tubes in compression $KL/r \leq 2.1\sqrt{(E/F_y)}$	$0.25\Delta_c$	$4\Delta_c$	$6\Delta_c$
Slender HSS, Pipes, Tubes in compression $KL/r \geq 4.2\sqrt{(E/F_y)}$	$0.25\Delta_c$	$5\Delta_c$	$7\Delta_c$
Intermediate HSS, Pipes, Tubes in compression	Linear Interpolation		
HSS, Pipes, Tubes in tension	$0.25\Delta_T$	$7\Delta_T$	$9\Delta_T$

a. IO, i.e., Immediate Occupancy
b. LS, i.e., Life Safety
c. CP, i.e., Collapse Prevention

It should be noted that the deformation capacities given in Table.2 are obtained for highly ductile braces or grout-filled ones. As discussed, the occurrence of local buckling depends on the width-to-thickness ratio; however, considerable impact of width-to-thickness ratio is not appropriately taken into account in ASCE 41 (2007).

FE ANALYSES AND VERIFICATION

Cyclic behaviour of tubular braces has been studied in both experiments and analyses. Haddad (2004) developed FE models utilizing shell elements for discretising the geometry. Fell (2008) employed cyclic void growth model (CVGM) for simulating fracture initiation in braces. Other investigators have developed FE models to study the cyclic behaviour as well (Yoo et al 2007; Takeuchi and Matsui 2011; Kuşyılmaz and Topkaya 2011).

In this paper, FE analyses were carried out to investigate the behaviour of steel braces subjected to cyclic loadings. Four specimens including two pipes and two square hollow structural shapes (SHHS) tested by Fell (2008) were used to verify analyses. Table.3 presents the geometric properties of FE models. Comparing the forgoing AISC's limit with the geometric properties given in Table.3, it can be concluded that all specimens satisfy the limits for investigating as SCBFs.

Table 3. Geometric properties of FE models

Specimen	Referring specimen	Section (mm)	Yield stress (MPa)	Length, L (mm)	Thickness, t (mm)	D/t, or W/t	L/r
Pipe-1	P-1-2	Pipe 127STD	351	3060	6.5	20.5	64.2
Pipe-2	P-2-2	Pipe 76STD	379	3060	5.5	14.8	103.8
SHSS-1	HSS1-1	SHSS 101.6	503	3061	6.4	15.9	73.7
SHSS-2	HSS2-1	SHSS 101.6	441	3061	9.5	10.7	73.4

Abaqus (2010) was utilized to simulate these four specimens. Structured mesh was generated for discretising the geometry. S4R elements with five integration point across the thickness were assigned to the geometry. Finer mesh size was generated at the mid-span to achieve sufficient accuracy, as shown in Fig. 1.

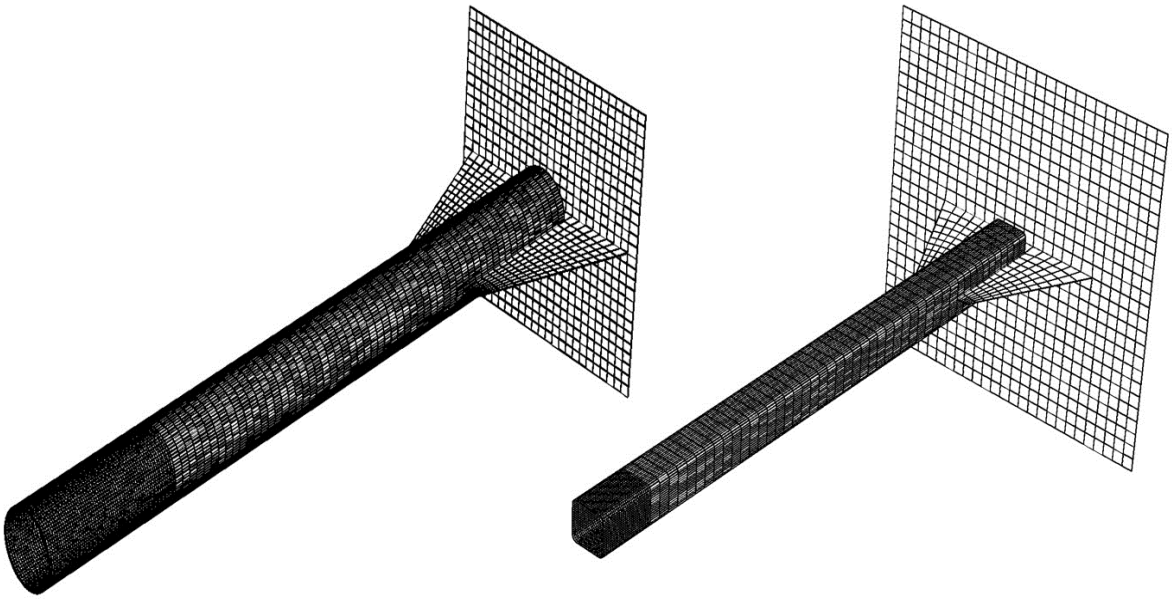

Figure 1. An illustration of specimens Pipe-1 and SHSS-1 [half of FE models are depicted]

Elastic behaviour of material was introduced to the FE models by assuming modulus of elasticity and poisson's ratio equal to 200GPa and 0.3, respectively. Combined nonlinear isotropic and kinematic hardening model was considered for work hardening behaviour in which both movement and growth of Von-Mises yield surface were included. It should be noted that the combined hardening model simulates Bauschinger effect appropriately. Material parameters were assumed based on what were obtained by Myers et al. (2010).

First mode shape of linear buckling analysis is employed to introduce initial imperfections to FE models. One-thousandth of the length of specimens (L/1000) was considered as amplitude for nodal displacement of the first buckling mode shape to define the initial imperfections.

Fig. 2 shows the cyclic loading protocol exerted at one end similar to what was conducted in experiments (Fell 2008). In all analyses, members were assumed to perform pine-ended. Static analysis accompanied by Full Newton method was utilized to solve nonlinear equations.

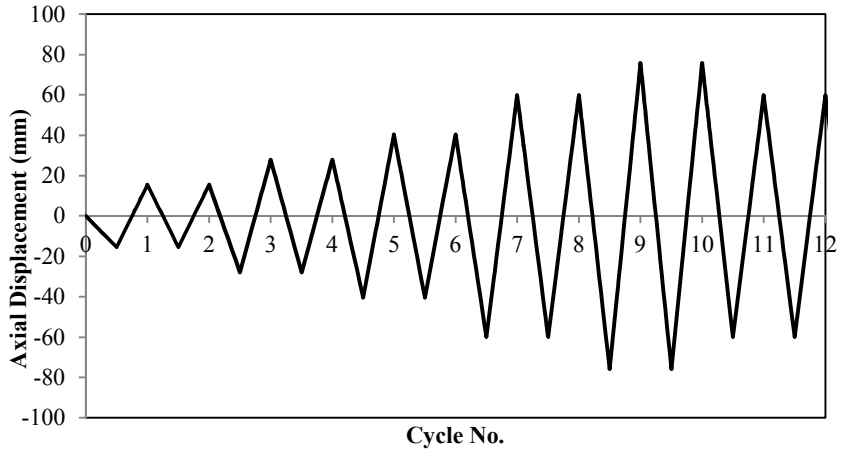

Figure 2. Cyclic loading protocol from Fell (2008)

In order to obtain verification for FE models, a comparison between analytical hysteresis curves and experimental ones was drawn. Fig.3 illustrates good agreement between analytical hysteresis curves and experimental ones. As shown in this figure, load carrying capacity of braces in compression drops after the overall buckling. Moreover, the axial load corresponding to the overall

buckling reduces as the cycle's number increases. This reduction might result from Bauschinger effect that was simulated fairly accurate. In addition, it should be noticed that analyses are capable of predicting tensile behaviour rather precise.

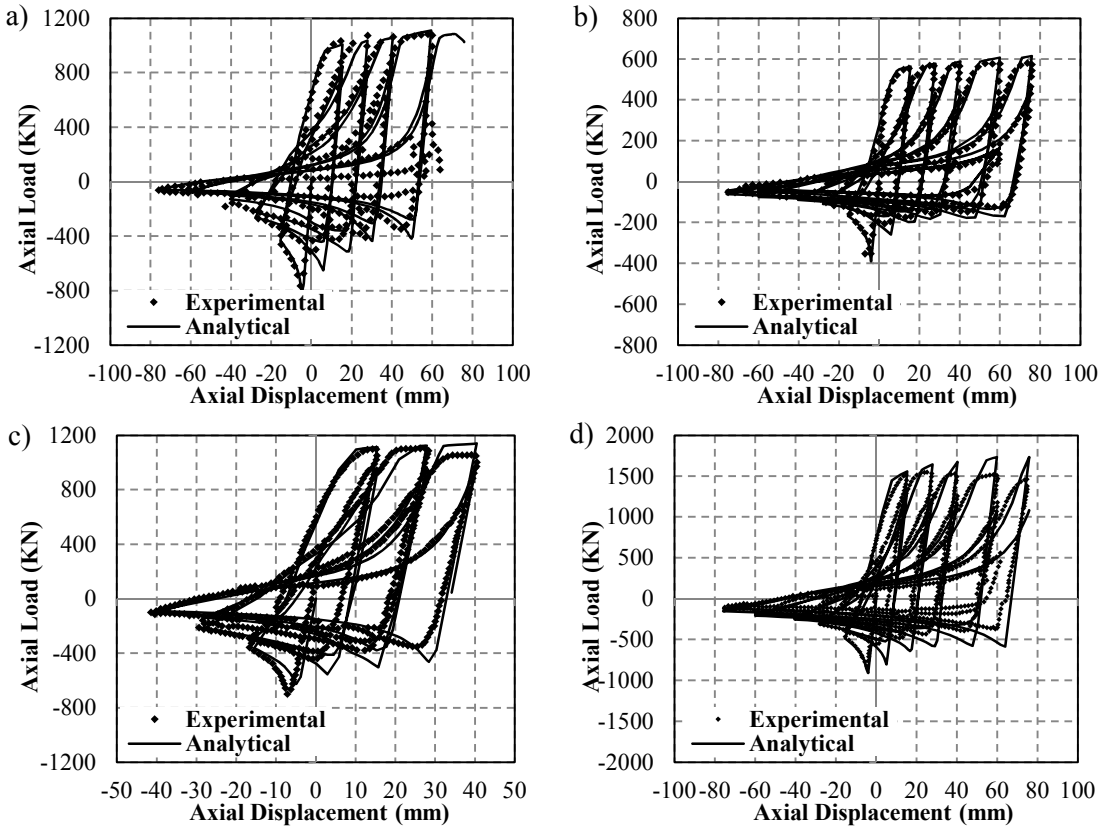

Figure 3. Hysteretic behaviour of specimen a) Pipe-1 b) Pipe-2 c) SHSS-1 d) SHSS-2 (Experimental data were obtained from Fell 2008)

COMBINED BUCKLING

FE analyses demonstrate that braces remain straight as long as the overall buckling has not happened. As the overall buckling occurs, the brace starts to deflect out-of-plane, and central part undergoes a flexural moment in addition to exerted axial compression loading. Plastic strains will be accumulated at the mid-span, and therefore, a plastic hinge forms at the central part of the member. However, the deflection almost disappears as the member undergoes tensile loading.

Accumulation of plastic strain at the mid-span triggers the local buckling at the central plastic hinge. Since in compacted members the local buckling does not precede the overall buckling, and is initiated due to the combined compression and bending; this mechanism can be entitled as combined buckling. However, it should be noticed that such mechanism might not be observed in braces that the local buckling occurs prior to the overall buckling.

Fig.4 depicts the combined buckling mechanism. Referring to this figure, it can be observed that in both ends of the member at which gusset plates were connected to the brace, plastic hinges were formed as well. This figure draws a comparison between deformed shape of braces prior to, and after the local buckling. The deformed shape is similar to a half-sine curve prior to the local buckling. However, as the brace experiences the local buckling, the overall deformed shape considerably transforms into two broken lines. This trend was previously observed by Tremblay (2002).

As a result, it can be concluded that FE models are capable of simulating and predicting the formation of plastic hinges, the overall and local buckling, yielding, and the deformed shape with reasonable accuracy.

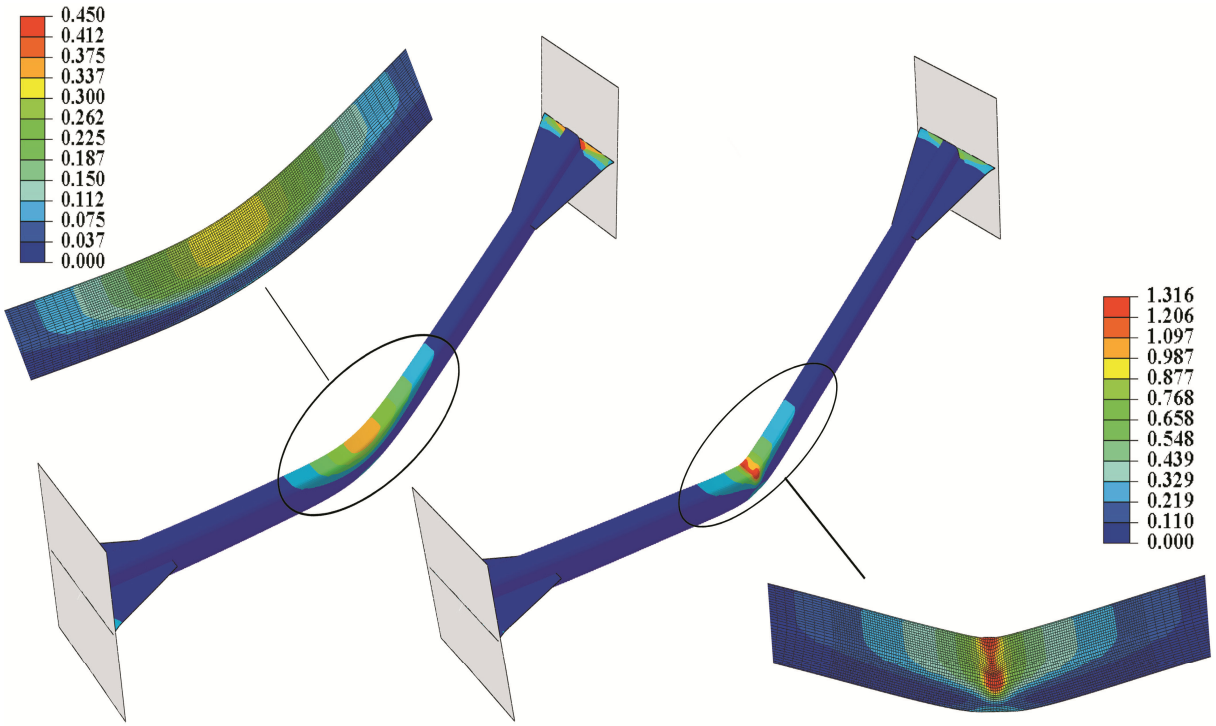

Figure 4. Combined buckling mechanism [Equivalent plastic strain contours]

OCCURRENCE OF LOCAL BUCKLING

FE analyses revealed that as long as the local buckling has not occurred, elements located at the mid-span experience a gradual increase in plastic strain. However, the local buckling induces a noticeable change in deformed shape accompanied by a distinctive divergence in strain pattern. Kuşyılmaz and Topkaya (2011) specified local buckling initiation as local strains of two adjacent nodes located at the mid-span, start showing considerably different values. Likewise, Takeuchi and Matsui (2011) observed a similar diverging pattern in plastic strains shell layers in the element located at local buckling region. Fig.5 shows local plastic strain in the element located at the mid-span. According to this figure, plastic strain of the inner and outer layers departs instantly in a specific point. Analyses represent that this point corresponds to the geometric changes after the local buckling. Therefore, it can be concluded that the main origin of divergence in strain pattern is the occurrence of local buckling.

In this paper, this noticeable change in strain pattern is adopted to define the occurrence of local buckling shown in Fig. 6. Table.4 compares the cycle in which local buckling occurs as well as reporting local buckling in experiments by Fell (2008). As presented, analyses predict the local buckling fairly accurate.

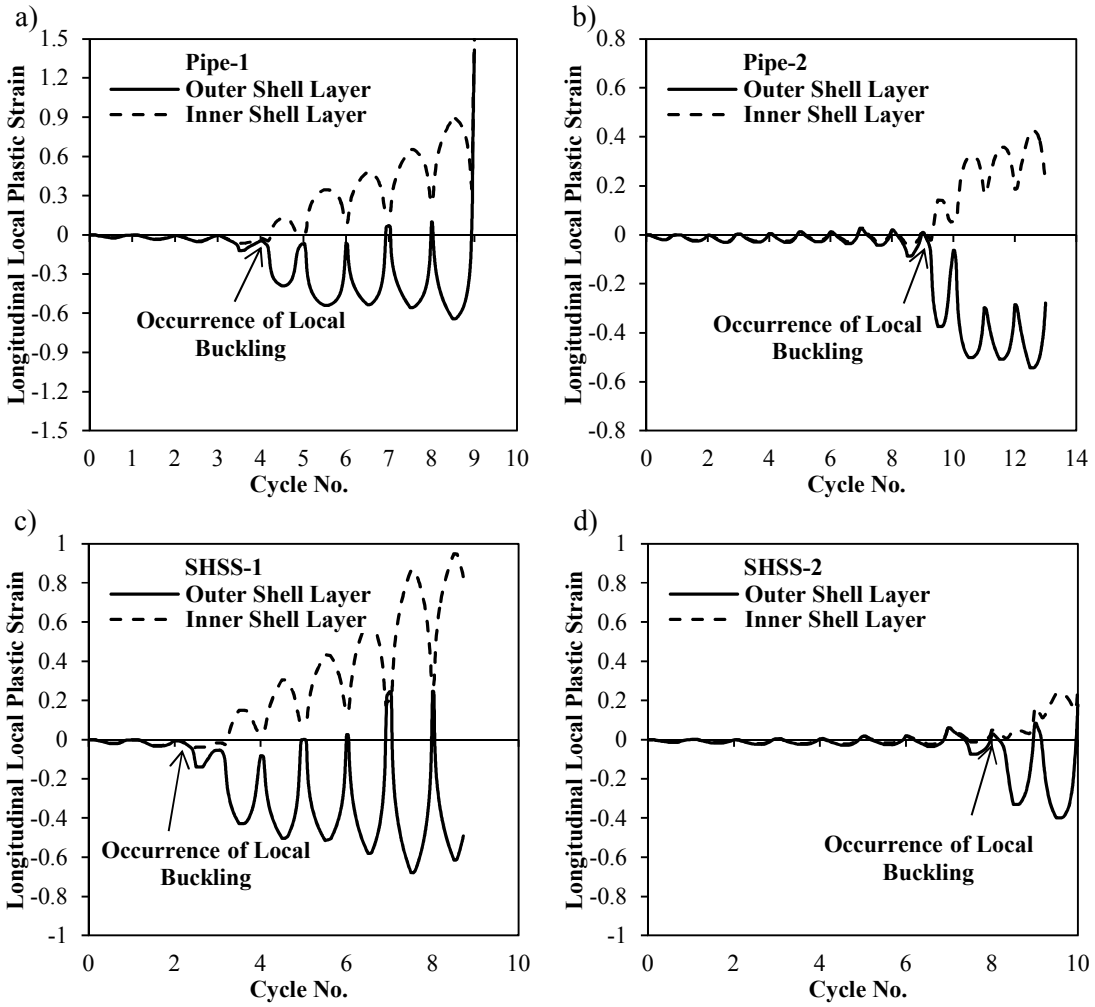

Figure 5. Local strain of shell layers in the element located at the mid-span for specimen a) Pipe-1 b) Pipe-2 c) SHSS-1 d) SHSS-2

STRAIN CONCENTRATION

Measurements of the strain at the mid-span plastic hinge demonstrate a sharp rise after the occurrence of local buckling. This severe growth of strain results in rupture failure at the mid-span plastic hinge, as confirmed by general observations in experiments (Han et al. 2007; Takeuchi and Matsui 2011; Shaback and Brown et al. 2003). Fig.6 shows equivalent plastic strain at the mid-span prior to, and after the occurrence of local buckling. As shown, equivalent plastic strain gradually increases prior to the local buckling. However, it grows significantly after the occurrence of local buckling that might be attributed to geometric changes. Note that the plastic strain of outer shell layer rises sharply in comparison with the inner layer. As a result, the occurrence of local buckling can be identified as the major event that causes a rupture failure at the mid-span. In general, the local buckling can be introduced as the main limit state that can be used as an index for evaluation of the overall deformation capacity of braces.

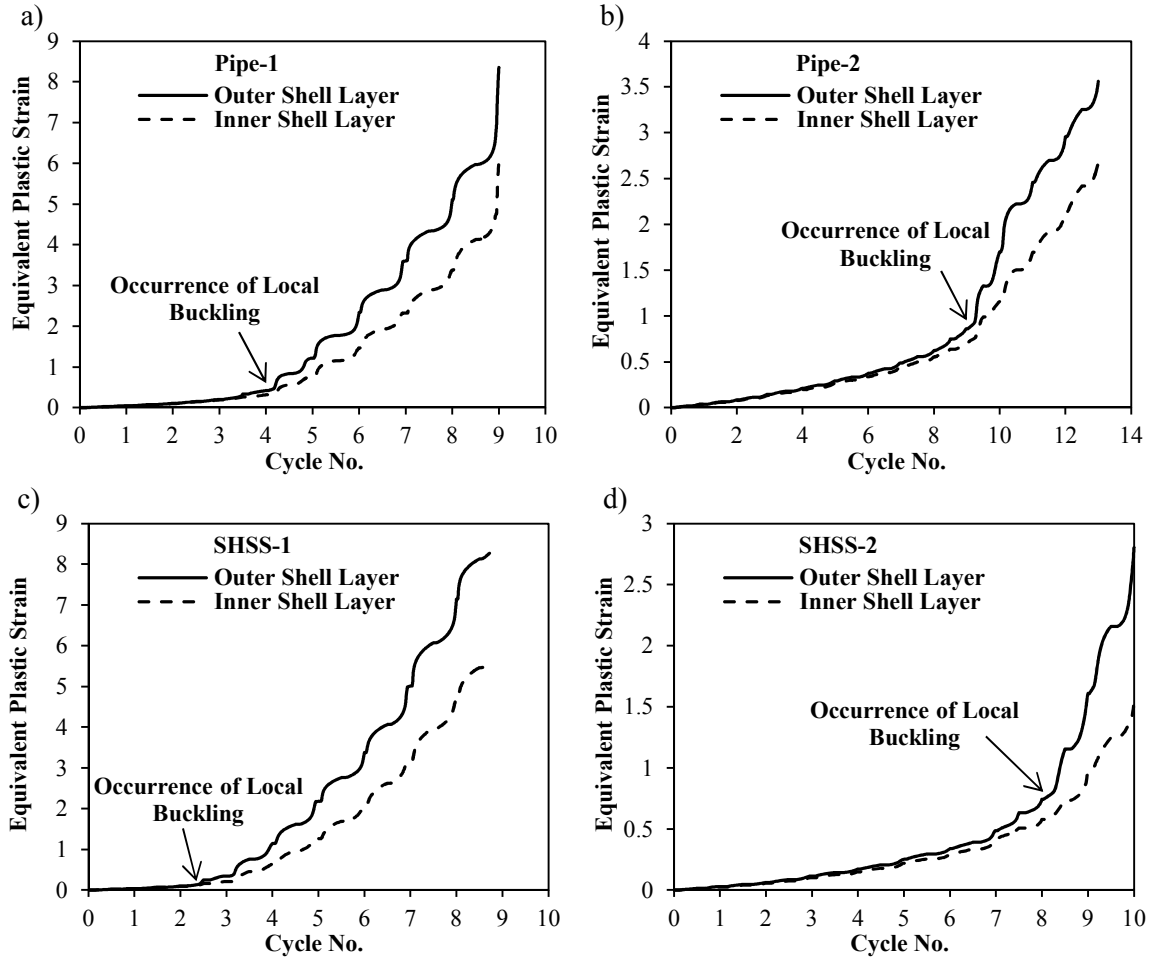

Figure 6. Strain rise after the occurrence of local buckling for specimen a) Pipe-1 b) Pipe-2 c) SHSS-1 d) SHSS-2

DETERIORATION DUE TO CYCLIC LOADING

As discussed, local buckling can be considered as a limit state for evaluation of deformation capacity. In order to study cyclic loading effects, the forgoing specimens were subjected to monotonic compression in addition to cyclic loading. The global strains corresponding to the local buckling are presented in Table.4. As presented, cyclic loadings decrease the local buckling strains to one-fifth of its values under compression loading. Therefore, cyclic loading deteriorates and makes a substantial impact on the deformation capacity of tubular braces.

Table 4. Prediction of local buckling

Specimens	Occurrence of local buckling				
	Cycle No.		Global strain		
	Experiment	Analysis	Cyclic	Monotonic	Cyclic/Monotonic (%)
Pipe-1	5	5	0.0044	0.0227	19.3
Pipe-2	10	10	0.0127	0.0578	22.0
SHSS-1	4	3	0.0031	0.0140	22.1
SHSS-2	9	9	0.0165	0.0717	23.0

CONCLUSIONS

Assessment of ASCE 41 (2007) recommendations demonstrates that effective parameters on deformation capacity of braces were not appropriately taken into account. It seems that width-to-thickness ratio and slenderness ratio greatly affect the deformation capacity of braces. In addition, FE analyses were carried out on four tubular braces previously tested by other investigators. The following conclusions can be made:

- FE models are capable of simulating and predicting the formation of plastic hinges, the overall and local buckling, yielding, and the deformed shape with reasonable accuracy.
- The combined action of bending and compression resulted from the overall buckling triggers the local buckling at the mid-span.
- A noticeable difference in local strains of outer and inner shell layers arise when the local buckling occurs. This index can be employed for identification of the occurrence of local buckling.
- Plastic strain rise sharply after the local buckling that may result in the rupture failure of braces. Thus, the local buckling can be introduced as the main cause of rupture that substantially affects the deformation capacity.
- Cyclic loading severely deteriorates the deformation capacity of braces.

REFERENCES

Abaqus, Inc. (2010) Abaqus/CAE User's Manual.

American Institute of Steel Construction, AISC 341 (2010) Seismic provisions for structural steel buildings, Chicago.

ASCE/SEI Seismic Rehabilitation Standards Committee (2007) Seismic Rehabilitation of Existing Buildings, ASCE/SEI 41-06, American Society of Civil Engineers, Reston, VA.

Astaneh-Asl A, Goel S C, Hanson R D (1985) "Cyclic Out-of-plane Buckling of Double-angle Bracing", *Journal of Structural Engineering*, 111(5), 1135–1153.

Elchalakani M, Zhao XL, Grzebieta R (2003) "Tests of Cold-formed Circular Tubular Braces under Cyclic Axial Loading", *Journal of Structural Engineering*, 129(4), 507–514.

Haddad M (2004) Design of concentrically braced steel frames for earthquakes, Ph.D. thesis, Department of Civil Engineering, University of Calgary, Calgary, Alberta.

Han S, Kim T, Foutch A (2007) "Seismic Behaviour of HSS Bracing Members according to Width–Thickness Ratio under Symmetric Cyclic Loading", *Journal of Structural Engineering*, 133(2), 264–273.

Fell V, (2008) Large-scale Testing and Simulation of Earthquake-induced Ultra-low Cycle Fatigue in Bracing Members Subjected to Cyclic Inelastic Buckling, Doctoral dissertation, University of California.

Kuşyılmaz A and Topkaya C (2011) "A Numerical Study on Local buckling and Energy dissipation of CHS Seismic Bracing", *Thin-Walled Structures*, 49(8), 984–996

Myers A T, Deierlein G G, Kanvinde A M (2009) Testing and Probabilistic Simulation of Ductile Fracture Initiation in Structural Steel Components and Weldments, Stanford University, No 170.

Takeuchi T and Matsui R (2011) "Cumulative Cyclic Deformation Capacity of Circular Tubular Braces under Local Buckling", *Journal of Structural Engineering*, 137(11), 1311-1318.

Tremblay R, Archambault MH, Filiatrault A (2003) "Seismic Response of Concentrically Braced Steel Frames Made with Rectangular Hollow Bracing Members", *Journal of Structural Engineering*, 129(12).

Tremblay R (2002) "Inelastic Seismic Response of Steel Bracing Members", *Journal of Constructional Steel Research*, 58(5–8), 665–701.

Shaback B and Brown T (2003) "Behavior of Square Hollow Structural Steel Braces with End Connections under Reversed Cyclic Axial Loading", *Canadian Journal of Civil Engineering*, 30(4), 745–753.

Yoo JH, Roeder C W, Lehman D E (2008) "Analytical Performance Simulation of Special Concentrically Braced Frames." *Journal of Structural Engineering*, 134(6), 881–889.